RESEARCH ARTICLE

J Anim Sci Technol 2026;68(4):1083-1098
https://doi.org/10.5187/jast.2600012

JAST
Journal of Animal Science and Technology
pISSN 2672-0191 eISSN 2055-0391

Alterations in steroid hormone receptors, angiogenic, cell proliferation, apoptotic, and Ras-related factors during estrous cycle in porcine corpus luteum

Hyewon Kim[1], Sang-Hee Lee[1,2]*

[1]*College of Animal Life Sciences, Kangwon National University, Chuncheon, Korea*
[2]*School of Information and Communication Technology, University of Tasmania, Hobart, Australia*

Received: Jan 15, 2026
Revised: May 13, 2026
Accepted: May 16, 2026

***Corresponding author**
Sang-Hee Lee
E-mail: sang1799@kangwon.ac.kr

Copyright © 2026 Korean Society of Animal Science and Technology. This is an Open Access article distributed under the terms of the Creative Commons Attribution Non-Commercial License (http://creativecommons.org/licenses/by-nc/4.0/) which permits unrestricted non-commercial use, distribution, and reproduction in any medium, provided the original work is properly cited.

ORCID
Hyewon Kim
https://orcid.org/0009-0007-2496-8912
Sang-Hee Lee
https://orcid.org/0000-0001-8725-4174

Competing interests
No potential conflict of interest relevant to this article was reported.

Funding sources
This work was supported by Innovative Human Resource Development for Local Intellectualization program through the Institute of Information & Communications Technology Planning & Evaluation (IITP) grant (IIPT-2026-RS-2023-00260267) and 2023 Research Grant from Kangwon National University.

Abstract

This study aimed to examine the association of Ras signaling with steroid hormone receptors, angiogenic factors, cell cycle/cell proliferation markers, and apoptotic factors during the estrous cycle in pigs. Porcine corpus luteum (CL) tissues were classified into the early (EP), middle (MP), and late phases (LP). Furthermore, the mRNA and protein expression profiles of steroid hormone receptors, angiogenic factors, cell cycle-related factors, apoptosis-related factors, Ras and Ras GTPases were assessed using reverse transcription-polymerase chain reaction, western blot, and protein-protein interaction. The CL showed the highest tissue weight in the MP. At the mRNA level, *3β-HSD* and *P4R* were substantially increased at MP, and *PGF2αR* was markedly elevated at LP. At the protein level, 3β-HSD was the highest at MP, P4R was increased at EP, and PGF2αR was the highest at LP. For angiogenic factors, *angiopoietin 1* and *Tie2* mRNA levels were increased in MP, vascular endothelial growth factor D protein levels were increased in MP. Cell cycle factors revealed increased *extracellular signal-regulated kinase 1*, *cyclin dependent kinase 1*, and *cyclin B1* mRNA expression in MP, whereas CCNB1 protein expression increased in EP. *tumor necrosis factor receptor 1* mRNA was the highest in LP, *Bax* and *caspase 3* mRNA increased in the MP group, and *Bcl2* mRNA increased at EP. At the protein level, Casp3 was markedly increased in LP. Additionally, the Ras family and Ras GTPases showed stage-dependent expression alterations at the mRNA and protein levels. Search Tool for the Retrieval of Interacting Genes-based molecular action analysis suggested a conserved interaction architecture across species and indicated potential functional linkages connecting hormone receptors and angiogenesis modules with Ras-related components and downstream cell cycle factors. Thus, porcine CL reveals coordinated, phase-dependent alterations in steroidogenic activity, angiogenesis, cell cycle regulation, apoptosis, and Ras-related signaling components during the estrous cycle. In conclusion, these findings provide foundational evidence that Ras signaling pathways act as integrative regulatory modules linking endocrine and vascular cues to intracellular signaling during the estrous cycle. This supports further porcine-specific mechanistic studies to clarify the Ras-centered regulation of CL function.

Keywords: Angiogenesis, Apoptosis, Corpus luteum, Pigs, Ras GTPase

Acknowledgements
Not applicable.

Availability of data and material
Upon reasonable request, the datasets of this study can be available from the corresponding author.

Authors' contributions
Conceptualization: Lee SH.
Data curation: Kim H, Lee SH.
Formal analysis: Kim H.
Methodology: Kim H.
Software: Kim H.
Validation: Kim H.
Investigation: Kim H, Lee SH.
Writing - original draft: Kim H, Lee SH.
Writing - review & editing: Kim H, Lee SH.

Ethics approval and consent to participate
The Institutional Animal Care and Use Committee of the Kangwon National University approved all animal procedures (KW-250716-2).

Declaration of generative AI
No AI tools were used in this article.

INTRODUCTION

The corpus luteum (CL), a transient endocrine gland formed following ovulation, plays a crucial role in regulating female reproductive functions by secreting progesterone (P4) [1]. The action of prostaglandin F2 alpha (PGF2α) secreted from the endometrium under estrogen stimulation causes the blood vessels distributed in the CL to constrict, if pregnancy does not occur. The activity of the cholesterol synthesis enzymes is suppressed, resulting in their degeneration [2]. In mammals, the CL is one of the few adult tissues that undergo rapid formation, functional maturation, and structural regression during each estrous cycle [3]. Dynamic remodeling involves extensive alterations in angiogenesis, cell proliferation, and apoptosis [4].

During the initial CL formation stage, ovulation triggers extensive vascular invasion, whereby blood vessels originating from the theca layer rapidly penetrate the ruptured follicles' granulosa compartment [5]. This newly established vascular network facilitates the efficient delivery of cholesterol and endocrine signals necessary for steroidogenesis [6]. Luteal cells differentiated from granulosa and theca cells synthesize P4 using cholesterol stored in the cytoplasmic lipid droplets, thereby supporting luteal endocrine function [7]. PGF2α secreted from the uterus disrupts luteal blood flow and steroidogenic activity in the absence of pregnancy, thereby initiating functional and structural luteal regression [8]. Consequently, the luteal tissue undergoes atrophy accompanied by lipid degeneration of luteal cells, ultimately forming the corpus albicans [9]. The integrative mechanisms coordinating angiogenesis, steroidogenesis, cell proliferation, and apoptosis during the estrous cycle in pigs remain elusive, although these regulatory components have been individually described.

Cell cycle progression and proliferation are fundamental processes that support rapid growth and functional establishment of the CL during the estrous cycle [10]. After ovulation, luteal cells actively proliferate to expand luteal tissue mass and acquire full steroidogenic capacity, a process tightly regulated by key cell-cycle–associated factors, including cyclin B1 (CCNB1), cyclin-dependent kinase 1 (CDK1), and the mitogen-activated protein kinases/extracellular signal-regulated kinase (MAPK/ERK) signaling components ERK1 and MAPK1 [11]. The activation of the MAPK/ERK pathway facilitates proliferation and differentiation of the luteal cell, thereby promoting luteal maturation and P4 production [11]. Contrastingly, dysregulation of this pathway disrupts folliculogenesis and luteinization [12]. As the estrous cycle advances, proliferative activity progressively declines and apoptotic signaling becomes dominant, driving structural and functional regression of the luteal cell [13]. The balance between pro-apoptotic factors (tumor necrosis factor receptor 1; TNFR1, Bax, and caspase 3; Casp3) and anti-apoptotic proteins, such as Bcl2, ultimately determines luteal cell survival and CL lifespan [14].

Ras and Ras guanosine triphosphatases (GTPases) are small GTP-binding proteins that act as molecular switches to control intracellular signaling associated with proliferation, differentiation, and survival [15]. Ras guanine nucleotide exchange factors (Ras GEFs), such as the son of sevenless homolog 1 (SOS1), mediate Ras activation whereas Ras GTPase-activating proteins (Ras GAPs), including neurofibromatosis type 1 (NF1) and Ras p21 protein activator 1 (RASA1), govern inactivation [16]. These regulatory proteins converge on major signaling cascades, such as the MAPK/ERK and PI3K/AKT-pathways known to affect ovarian follicular growth, steroid hormone production, angiogenesis, and cell-cycle regulation [17]. Although Ras-mediated signaling has been assessed in several reproductive tissues, studies particularly addressing Ras's role and its GTPases in porcine CL physiology remain limited. Considering the rapid structural alterations and high metabolic demands of the CL, Ras signaling may be a key integrative regulator linking angiogenesis, steroidogenesis, and cellular turnover [18].

However, Ras and its GTPases during the estrous cycle in porcine CL have not been clearly

https://doi.org/10.5187/jast.2600012

defined. No comprehensive investigation has been conducted to compare the expression of Ras family members (H-, K-, N-, and R-Ras) and their regulatory proteins across distinct estrous cycles. Additionally, the potential interactions among Ras GTPases, steroid hormone receptors, and angiogenic factors have not been examined in pigs. Understanding these molecular relationships is critical because Ras signaling pathways may affect the transition from proliferation and steroidogenesis in the early phase (EP) and middle phase (MP) to apoptosis and regression in the late phase (LP) [19].

Pigs and humans share key reproductive characteristics, including ovarian follicular dynamics, steroid hormone profiles, angiogenic mechanisms, and the balance between proliferative and apoptotic signals during the development and regression of CL [20,21]. These similarities improve the translational value of porcine studies for understanding human ovarian physiology, estrous cycle deficiency, and early pregnancy loss. From a practical perspective, elucidating the CL function in pigs contributes to improved reproductive management in the swine industry, supporting enhancements in estrous synchronization, fertility monitoring, and pregnancy diagnosis [22]. Additionally, the characterization of steroidogenesis, angiogenesis, and cell turnover in the porcine CL provides fundamental insights into the biology of a rapidly remodeling endocrine gland [23,24]. Thus, porcine CL research has agricultural and biomedical significance, strengthening its role as a model for mammalian reproductive physiology.

The angiogenic [25], steroidogenic [26], cell proliferation [27], and apoptotic [28] pathways are dynamically regulated during CL development and regression in pigs. Ras and its GTPases function as the primary molecular switches that control intracellular signaling associated with cell proliferation [29], differentiation [30], angiogenesis [31], and apoptosis [32,33] in different reproductive tissues. Considering these observations, together with the rapid structural remodeling and high metabolic demands of the CL, we hypothesized that Ras-related signaling pathways play an integrated role in coordinating luteal development and regression in pigs. We investigated the phase-dependent expression patterns of the Ras family members (H-, K-, N-, and R-Ras) and their regulatory proteins (NF1, RASA1, and SOS1) in the porcine CL during the EP, MP, and LP. Furthermore, we simultaneously examined the mRNA and protein expression levels of hormone receptors, angiogenic markers, cell cycle regulators, and apoptotic factors. Pathway-level protein–protein interaction (PPI) analysis was performed using the Search Tool for the Retrieval of Interacting Genes (STRING) database to further elucidate the molecular relationships underlying these regulatory processes. Additionally, we aimed to clarify the potential involvement of Ras-related signaling in integrating angiogenesis, steroidogenesis, cell proliferation, and apoptosis during the porcine estrous cycle.

MATERIALS AND METHODS

Animals and corpus luteum collection

The Institutional Animal Care and Use Committee of the Kangwon National University approved all animal procedures (KW-250716-2). Porcine CL were collected at a local slaughterhouse (Pocheon farm) and transported to the laboratory at 4℃ within 2 h following slaughter. The estrous cycle phase was assigned primarily based on ovarian and CL morphology in the laboratory (Figs. 1A, 1B, and 1C). The CL of EP were defined as samples showing visible red blood within the CL, having a relatively smaller overall size than MP CL, and showing blood inside the tissue after isolation and dissection (Fig. 1A). The CL of MP were defined as samples in which blood was not observed and which showed a pinkish luteal coloration (Fig. 1B). The CL of LP were defined as samples with a smaller tissue size than MP CL and ovaries containing developing follicles (Fig.

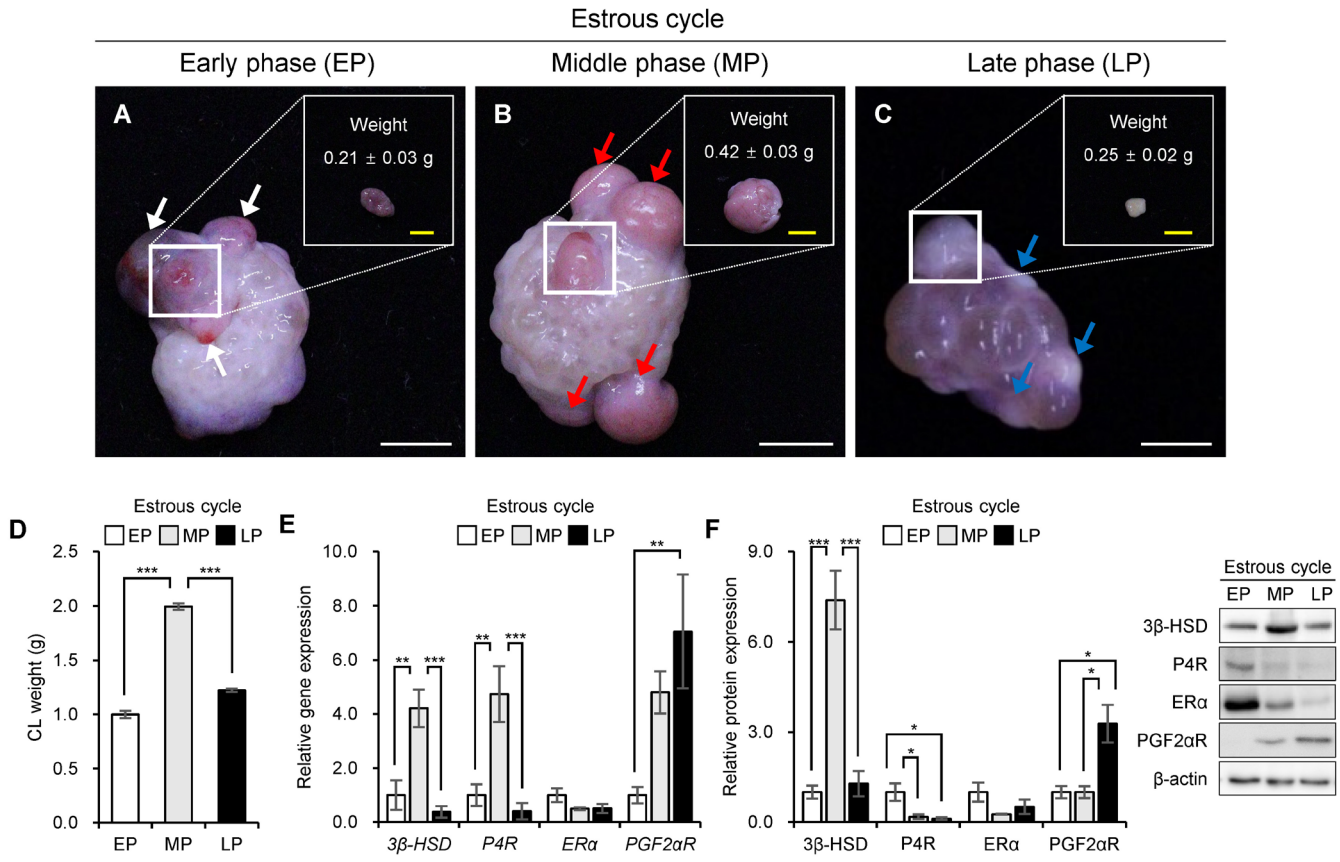


Fig. 1. Morphological characteristics, tissue weight, and expression of the steroid hormone receptors in the porcine ovary during the estrous cycle. Representative images revealing the shape of the prominent corpus luteum (CL) in porcine ovaries at the early (EP; A; white arrows), middle (MP; B; red arrows), and late phases (LP; C; blue arrows) of the estrous cycle. The white scale bar indicates 1.0 cm, and the yellow scale bar indicates 0.5 cm. White boxes represent enlarged areas of the CL. The tissue weight of the CL during the estrous cycle (D); alterations in *3β-hydroxysteroid dehydrogenase* (*3β-HSD*), *progesterone receptor* (*P4R*), *estrogen receptor alpha* (*ERα*), and *prostaglandin F2 alpha receptor* (*PGF2αR*) mRNA (E) and protein (F), mRNA and protein expression of the MP and LP was normalized to that of the EP. Data are presented as the mean ± SEM. Significant differences between groups are indicated as $^{*}p < 0.05$, $^{**}p < 0.01$, $^{***}p < 0.001$.

1C). The expression patterns of *3β-hydroxysteroid dehydrogenase* (*3β-HSD*) and *prostaglandin F2 alpha receptor* (*PGF2αR*) were examined only as supportive biological indicators of luteal functional status and were not used for marker-based reclassification of the samples (Figs. 1E and 1F). Subsequently, all isolated CL tissues were weighed and stored at −80℃ until further use.

RNA extraction and cDNA synthesis

Total RNA was extracted using RNAiso Plus (Takara Bio), according to the manufacturer's protocol. RNA quality and concentration were measured using an EzDrop 1000C spectrophotometer (Blue-Ray Biotech). Next, 5.0 μg RNA was utilized to synthesize cDNA using a SuPrimeScript cDNA Synthesis Kit (Genetbio) according to the manufacturer's instructions. Furthermore, cDNA was stored at −18℃ until reverse transcriptase polymerase chain reaction (RT-PCR).

Real-time PCR

Using a qPCR system (Quant3 Studio, Applied Biosystems, Thermo Fisher Scientific), cDNA, along with qPCR mix, primers, and ddH2O, was amplified. Amplification conditions included incubation at 50℃ for 2 min, initial denaturation at 95℃ for 10 min, followed by 40 cycles of

https://doi.org/10.5187/jast.2600012

denaturation at 95℃ for 15 s and annealing/extension at 60℃ for 1 min. The mRNA expression levels were normalized to that of *β-actin* mRNA. All reactions were performed in triplicate. Primer specificity was confirmed by melt curve analysis. Table 1 lists the primer sequences used in the experiments. We computed the relative mRNA expression levels using the comparative cycle threshold ($2^{-\Delta\Delta Ct}$) method [34].

Western blot

Luteal tissues were lysed in radio-immunoprecipitation assay cell lysis buffer (GenDEPOT) containing inhibitors (Xpert protease inhibitor cocktail solution and Xpert phosphatase inhibitor cocktail solution; GenDEPOT). The resulting homogenate was centrifuged at 12,000 rpm (13,523×g) and 4℃ for 20 min and the supernatants were collected in a fresh tube. Total protein concentration was measured using the Pierce Bicinchonic Acid Protein Assay Kit-Reducing Agent Compatible, according to the manufacturer's protocol (23250; Thermo Fisher Scientific). Proteins were separated using sodium dodecyl sulfate-polyacrylamide gel electrophoresis and transferred onto polyvinylidene difluoride membranes (Merck Millipore) using a Trans-Blot turbo rapid transfer system (1704150, Bio-Rad), according to the manufacturer's protocol. The membranes were blocked in blocking solution (5% skim milk in Tris-buffered saline/0.5% Tween-20; TBS-T) at room temperature for 1 h. After blocking membranes, the membranes incubated overnight at 4℃ with the appropriate primary antibodies (Table 2). Images were acquired using a chemiluminescence substrate (W3651-012; GenDEPOT) and quantified using a chemiluminescence imaging system (UVITEC Alliance MINI HD9 system, UVITEC). Band intensities were quantified by densitometric analysis and normalized to β-actin as a loading control.

Bioinformatics analysis

Protein–protein interaction and functional association networks were constructed using the STRING [35] (v.10.0; http://string.embl.de) database, with *Sus scrofa* selected as the target species. Network edges were generated using a medium confidence score cutoff of 0.400. The molecular action view was used to visualize predicted interaction modes, including positive and negative interactions, activation, and inhibition. STRING-derived interactions were interpreted as predicted functional associations rather than experimentally validated causal relationships. Subsequently, the molecular action of the Ras GTPases (NF1, RASA1, and SOS1), hormone receptors (progesterone receptor; P4R, prostaglandin F2 alpha receptor; PGF2αR, and estrogen receptor alpha; ERα), angiogenesis factors (vascular endothelial growth factor A; VEGFA, VEGF receptor 2; VEGFR2, angiopoietin 1; Ang1, and Tie2), apoptosis factors (TNFR1, Bax, and Casp3), and Ras proteins (H-Ras, K-Ras, N-Ras, and R-Ras) were examined using the STRING database.

Statistical analysis

Each experiment was conducted with at least three replications. Data was analyzed using SAS ver. 9.4 (SAS Institute). Data was presented as the mean ± SEM and differences between each group (EP vs MP, MP vs LP, and EP vs LP) were calculated using Student's t-test. Statistical significance was set at $p < 0.05$.

RESULTS

Morphological characteristics, tissue weight, and expression of the steroid hormone receptors in the porcine ovary during the estrous cycle

Fig. 1 shows the morphological characteristics of the porcine ovaries at the EP (Fig. 1A), MP (Fig.

Table 1. Primer condition for reverse transcriptase polymerase chain reactio (RT-PCR)

Genes	Sequence (5'-3')	Annealing temperature (℃)	Product size (bp)	Accession No.
3β-HSD	F: CCTTCCTGCTGGAAATAGTG	60	112	NM_001004049.2
	R: TCTTGTAGGAGACGGTGAA			
P4R	F: GGACTAGGATGGAGATCCTATAA	60	124	NM_001166488.1
	R: GCCACATGGTAAGGCATAA			
ERα	F: CTACCCTCTGTGACCTCTTC	60	144	NM_001170521.1
	R: CCACACCCAACACCAATAC			
PGF2αR	F: GCCATCACGGGAATTTCA	60	117	NM_214059.1
	R: GCAGGAGACGCACATTATAG			
VEGFA	F: CAACTTCTGGGCTGTTCTC	60	147	NM_001435273.1
	R: CCTCTCCTCTTCCTTCTCTT			
VEGFR2	F: TGTCCTGCTCTGGGAAATA	60	146	XM_013997943.2
	R: CAAGCATCGTCTGGTACATC			
Ang1	F: GAAGGAAACCGAGCCTATTC	60	91	NM_213959.1
	R: TCCCACTGTGACCCTTTA			
Tie2	F: GACGTGTGCAGAACTCTATG	60	102	XM_021062688.1
	R: CGCCAGCATTGTCTCATAA			
H-Ras	F: CCCTGACCATCCAGCTTAT	60	89	XM_021082554.1
	R: GTCAATGACCACTTGCTTCC			
K-Ras	F: GATGGAGAAACCTGTCTCTTGG	60	80	XM_005653151
	R: CTCATGTACTGGTCCCTCATTG			
N-Ras	F: TCCCACCATAGAGGACTCTTAC	60	130	NM_001044537.1
	R: TTCGCCTGTCCTCATGTATTG			
R-Ras	F: CCTGCTGGTGTTTGCCATTA	60	94	XM_003355998.3
	R: GAAGTCATCTCGGTCCTTGACT			
RASA1	F: TCCAGAACAAGCAGAGGATTG	60	97	XM_021084515.1
	R: GACCTGACGCAGACGTTTAT			
SOS1	F: TCCTCCTGCTTCTGGTGCTTCTAG	60	210	XM_021087589.1
	R: AAAGACGGTATCGCTGCTTGAGTG			
NF1	F: GCAGTTCAGACCCTAGTTTAC	60	123	XM_021067460.1
	R: TGTTGGCTGGGATACATAACC			
ERK1	F: CCACATCTGCTACTTCCTCTAC	60	196	HM745137
	R: GGCCACATATTCCGTCAAGA			
MAPK1	F: CCCTCACAAGAGGATTGAAGTAG	60	189	NM_001198922
	R: GATCTGTATCCTGGCTGGAATC			
CDK1	F: GGTGTTCCTAGTACTGCCATTC	60	179	NM_001159304.2
	R: GAATCCATGAACTGACCAGGAG			
CCNB1	F: GTGTCAGGCTTTCTCTGATGT	60	199	NM_001170768.1
	R: CCAGTCAATTAGGATGGCTCTC			
TNFR1	F: GAACGCAGACTGCAAGAA	60	137	NM_213969.1
	R: CTAAGCCAACGAAGAGGAAG			
Bax	F: CTCAGGATGCATCTACCAAGAA	60	213	XM_003127290.5
	R: GCACCAGTTTACTGGCAAAG			
Bcl2	F: AGGGCATTCAGTGACCTGAC	60	193	XM_021077293.1
	R: CGATCCGACTCACCAATACC			
Casp3	F: ACCGAAAGGTAGCAGTAGA	60	91	NM_214131.1
	R: GTGAGCATGGACACAATACA			
β-actin	F: TCTGGCACCACACCTTCTA	60	102	XM_021086047.1
	R: TCTTCTCACGGTTGGCTTTG			

3β-HSD, *3β-hydroxysteroid dehydrogenase*; *Ang1*, *angiopoietin 1*; *Bax*, *B-cell lymphoma 2-associated X protein*; *Bcl2*, *B-cell lymphoma 2*; *CCNB1*, *cyclin B1*; *CDK1*, *cyclin-dependent kinase 1*; *Casp3*, *caspase 3*; *ERK1*, *extracellular signal-regulated kinase 1*; *ERα*, *estrogen receptor alpha*; *H-Ras*, *Harvey rat sarcoma viral oncogene homolog*; *K-Ras*, *Kirsten rat sarcoma viral oncogene homolog*; *MAPK1*, *mitogen-activated protein kinase 1*; *N-Ras*, *Neuroblastoma rat sarcoma viral oncogene homolog*; *NF1*, *neurofibromin 1*; *P4R*, *progesterone receptor*; *PGF2αR*, *prostaglandin F2 alpha receptor*; *RASA1*, *RAS p21 protein activator 1*; *R-Ras*, *related RAS viral oncogene homolog*; *SOS1*, *son of sevenless homolog 1*; *Tie2*, *tyrosine kinase with immunoglobulin-like and EGF-like domains 2*; *TNFR1*, *tumor necrosis factor receptor 1*; *VEGFA*, *vascular endothelial growth factor A*; *VEGFR2*, *vascular endothelial growth factor receptor 2*; *β-actin*, *beta-actin*.

https://doi.org/10.5187/jast.2600012

Table 2. List of antibodies for western blot

1st Antibody (Ab)	Cat. No.	Host species	Company	1st Ab dilution	Secondary antibody	2nd Ab dilution
3β-HSD	sc-515120	Mouse	SCBT	1:1000	goat anti-mouse IgG-HRP	1:10000
P4R	sc-539	Rabbit	SCBT	1:1000	goat anti-rabbit IgG-HRP	1:10000
ERα	sc-8005	Mouse	SCBT	1:1000	goat anti-mouse IgG-HRP	1:10000
PGF2αR	sc-33364	Goat	SCBT	1:1000	donkey anti-goat IgG-HRP	1:10000
VEGF-D	sc-25784	Rabbit	SCBT	1:1000	goat anti-rabbit IgG-HRP	1:10000
Ang-4	sc-377497	Mouse	SCBT	1:1000	goat anti-mouse IgG-HRP	1:10000
Tie-2	sc-293414	Mouse	SCBT	1:1000	goat anti-mouse IgG-HRP	1:10000
ERK1/2	4696S	Mouse	Cell Signaling	1:2000	goat anti-mouse IgG-HRP	1:10000
p-ERK1/2	4370S	Rabbit	Cell Signaling	1:2000	goat anti-rabbit IgG-HRP	1:10000
CCNB1	554178	Mouse	BD	1:1000	goat anti-mouse IgG-HRP	1:10000
TNFR1	sc-8436	Mouse	SCBT	1:1000	goat anti-mouse IgG-HRP	1:10000
Bax	sc-23959	Mouse	SCBT	1:1000	goat anti-mouse IgG-HRP	1:10000
Bcl2	sc-7382	Mouse	SCBT	1:1000	goat anti-mouse IgG-HRP	1:10000
Casp3	sc-56046	Mouse	SCBT	1:1000	goat anti-mouse IgG-HRP	1:10000
H-Ras	sc-35	Rat	SCBT	1:1000	goat anti-rat IgG-HRP	1:10000
K-Ras	#71835	Rabbit	Cell Signaling	1:1000	goat anti-rabbit IgG-HRP	1:10000
R-Ras	#8446	Rabbit	Cell Signaling	1:1000	goat anti-rabbit IgG-HRP	1:10000
NF1	#14623	Rabbit	Cell Signaling	1:1000	goat anti-rabbit IgG-HRP	1:10000
RASA1	EP536Y	Rabbit	Abcam	1:1000	goat anti-rabbit IgG-HRP	1:10000
SOS1	#5890	Rabbit	Cell Signaling	1:1000	goat anti-rabbit IgG-HRP	1:10000
β-Actin	sc-47778	Mouse	SCBT	1:1000	goat anti-mouse IgG-HRP	1:10000

3β-HSD, 3β-hydroxysteroid dehydrogenase; Ang-4, angiopoietin 4; Bax, B-cell lymphoma 2-associated X protein; Bcl2, B-cell lymphoma 2; CCNB1, cyclin B1; Casp3, caspase 3; ERK1/2, extracellular signal-regulated kinase 1/2; ERα, estrogen receptor alpha; H-Ras, Harvey rat sarcoma viral oncogene homolog; HRP, horseradish peroxidase; IgG, immunoglobulin G; K-Ras, Kirsten rat sarcoma viral oncogene homolog; NF1, neurofibromin 1; P4R, progesterone receptor; PGF2αR, prostaglandin F2 alpha receptor; p-ERK1/2, phosphorylated extracellular signal-regulated kinase 1/2; RASA1, RAS p21 protein activator 1; R-Ras, related RAS viral oncogene homolog; SOS1, son of sevenless homolog 1; Tie-2, tyrosine kinase with immunoglobulin-like and EGF-like domains 2; TNFR1, tumor necrosis factor receptor 1; VEGF-D, vascular endothelial growth factor D.

1B), and LP (Fig. 1C) stages of the estrous cycle. The CL showed a substantial increase in size during the MP compared with that during the EP and LP. Consistent with these morphological observations, the tissue weight of the CL (Fig. 1D) was significantly higher in the MP than in the EP and LP ($p < 0.001$).

Figs. 1E and 1F show the relative expression levels of the steroid hormone receptors. At the mRNA level (Fig. 1E), the *3β-HSD* and *P4R* expressions were significantly increased at the MP compared with the EP and LP, whereas *ERα* mRNA expression did not significantly differ during the estrous cycle. Contrastingly, *PGF2αR* mRNA expression was significantly higher at the LP than at the EP and MP ($p < 0.05$). At the protein level (Fig. 1F), 3β-HSD protein expression was the highest at the MP, whereas P4R protein expression was elevated at the EP ($p < 0.001$). Similar to the mRNA results, ERα protein expression did not reveal significant differences among the stages, whereas PGF2αR protein expression was significantly increased at the LP ($p < 0.05$).

Expression of angiogenesis, cell cycle, and apoptosis-related factors

Figs. 2A, 2B, 2C, and 2D show the expression of the angiogenesis-and cell cycle-related factors in the porcine CL during the estrous cycle. The *VEGFA* and *VEGF receptor 2* (*VEGFR2*) mRNA expression levels (Fig. 2A) were not markedly different among the EP, MP, and LP groups. Contrastingly, the mRNA expression levels of *angiopoietin 1* (*Ang1*) and *Tie2* were significantly higher in the MP than in the EP and LP ($p < 0.05$). At the protein level (Fig. 2B), vascular

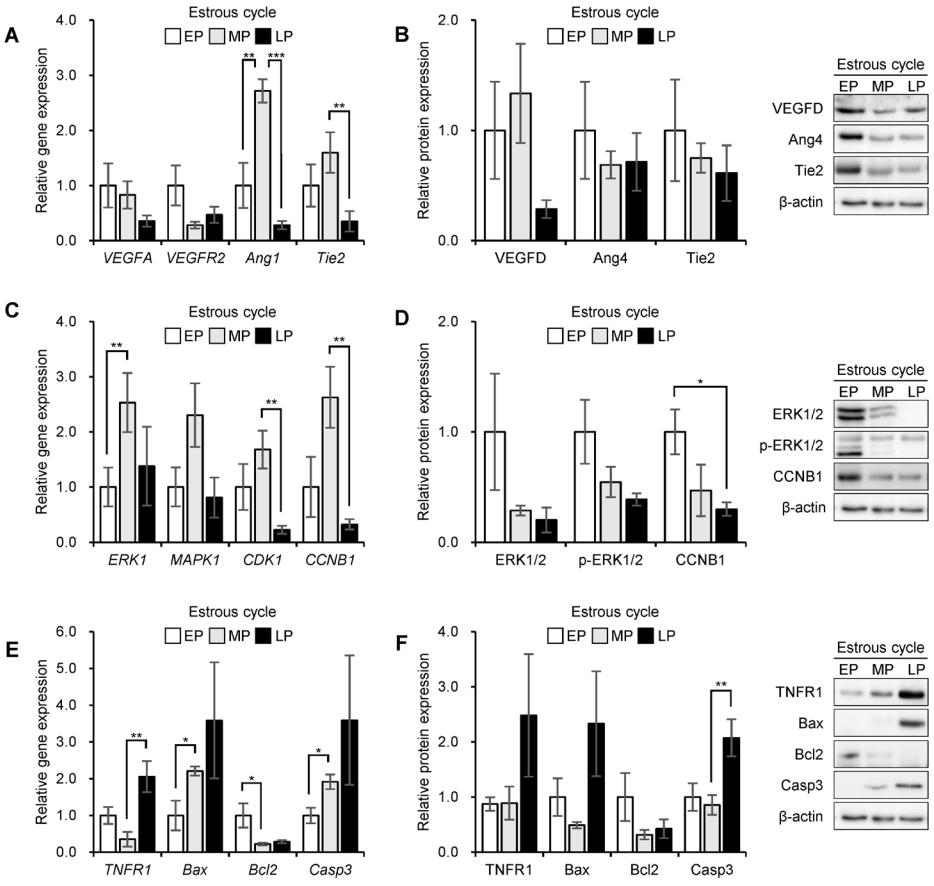


Fig. 2. Changes of angiogenic, proliferation, and apoptotic factors during estrous cycle in porcine corpus luteum. Changes in the *vascular endothelial growth factor A* (*VEGFA*), *vascular endothelial growth factor receptor 2* (*VEGFR2*), *angiopoietin 1* (*Ang1*), and *Tie2* mRNA (A); vascular endothelial growth factor-D (VEGFD), angiopoietin 4 (Ang4), and Tie2 protein (B); *extracellular signal-regulated kinase 1* (*ERK1*), *mitogen-activated protein kinase 1* (*MAPK1*), *cyclin-dependent kinase 1* (*CDK1*), and *cyclin B1* (*CCNB1*) mRNA (C); ERK1/2, phosphorylated ERK1/2 (p-ERK1/2), and CCNB1 protein (D); tumor necrosis factor receptor 1 (TNFR1), Bax, Bcl2, and caspase 3 (Casp3) mRNA (E) and protein (F) at the early (EP), middle (MP), and late phases (LP). mRNA and protein expression of the MP and LP was normalized to that of the EP. Data are presented as the mean ± SEM. Significant differences between the groups are indicated as $^{*}p < 0.05$, $^{**}p < 0.01$, $^{***}p < 0.001$.

endothelial growth factor D (VEGFD) protein expression was significantly higher at the MP than at the EP and LP ($p < 0.05$), whereas angiopoietin 4 (Ang4) protein expression did not significantly differ during the estrous cycle. Tie2 protein expression did not significantly differ during the estrous cycle. The mRNA expression levels of *ERK1*, *CDK1*, and *CCNB1* (Fig. 2C) were significantly higher in the MP group than in the EP and LP groups ($p < 0.05$), whereas *MAPK1* mRNA expression did not significantly differ during the estrous cycle. At the protein level (Fig. 2D), the expression levels of ERK1/2 and phosphorylated ERK1/2 (p-ERK1/2) were not significantly different among EP, MP, and LP, whereas CCNB1 protein expression was significantly higher in the EP than in the MP and LP ($p < 0.05$). Fig. 2E and 2F illustrate the expression patterns of the apoptosis-related factors. *TNFR1* mRNA expression levels (Fig. 2E) were significantly higher in the LP group than in the EP and MP groups ($p < 0.05$). Contrastingly, the mRNA expression levels of *Bax* and *Casp3* were significantly increased in MP, whereas *Bcl2* mRNA expression was significantly higher in EP than in MP and LP ($p < 0.05$). At the protein level (Fig. 2F), the expression levels of TNFR1, Bax, and Bcl2 were not significantly different during the estrous cycle, whereas Casp3 protein expression was

https://doi.org/10.5187/jast.2600012

significantly higher in the LP than in the EP and MP ($p < 0.05$).

Re-validation of the Ras family members and alterations in the Ras-related regulatory factors by mRNA and protein expression in the porcine corpus luteum

The expression of Ras family members and GTPases identified in the porcine CL was re-validated using mRNA and protein analyses (Fig. 3). The mRNA levels of *H-Ras*, *K-Ras*, *N-Ras*, and *R-Ras* were significantly changed during the estrous cycle (Fig. 3A). Compared to EP, the expression of Ras family mRNAs revealed significant alterations in MP and was significantly decreased in LP ($p < 0.05$). Similarly, the protein expression levels of H-Ras, K-Ras, and R-Ras were significantly altered during the estrous cycle, with higher expression noted in the MP and decreased expression in the LP than in the EP ($p < 0.05$; Fig. 3B). The mRNA expression levels of *NF1*, *RASA1*, and *SOS1* were not significantly different between the EP and MP, but were significantly changed in the LP ($p < 0.05$; Fig. 3C). At the protein level, the expression of NF1, RASA1, and SOS1 revealed significant stage-dependent alterations, with changed expression noted in the MP and LP compared to the EP ($p < 0.05$; Fig. 3D).

Molecular actions in the hormone receptors, angiogenesis, cell cycle, apoptosis, Ras GTPases, and Ras protein

Fig. 4 shows the molecular actions of hormone receptors, angiogenic factors, cell cycle-related factors, apoptotic factors, Ras GTPases, and Ras GTPase proteins. STRING-based molecular action networks were constructed using the same set of proteins arranged in the same positions

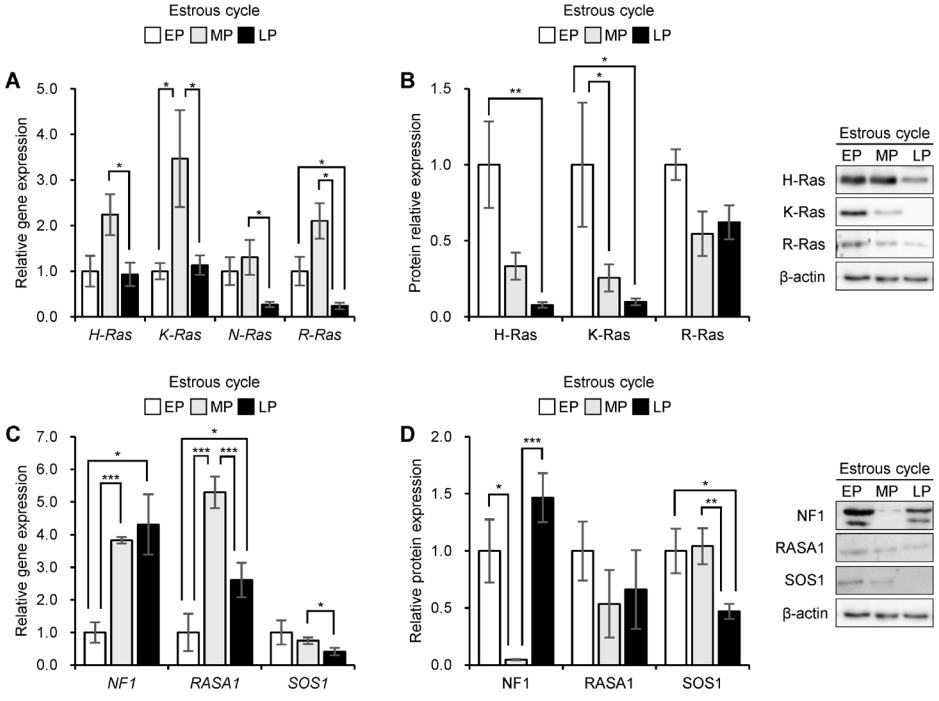


Fig. 3. Changes of Ras-related factors during estrous cycle in porcine corpus luteum. Changes in the *H-Ras*, *K-Ras*, *N-Ras*, and *R-Ras* mRNA (A); H-Ras, K-Ras, and R-Ras protein (B); neurofibromin 1 (NF1), Ras GTPase-activating protein 1 (RASA1), and son of sevenless homolog 1 (SOS1) mRNA (C) and protein (D) at the early (EP), middle (MP), and late phases (LP). mRNA and protein expression of the MP and LP was normalized to that of the EP. Data are presented as the mean ± SEM. Significant differences between the groups are indicated as $^{*}p < 0.05$, $^{**}p < 0.01$, $^{***}p < 0.001$.

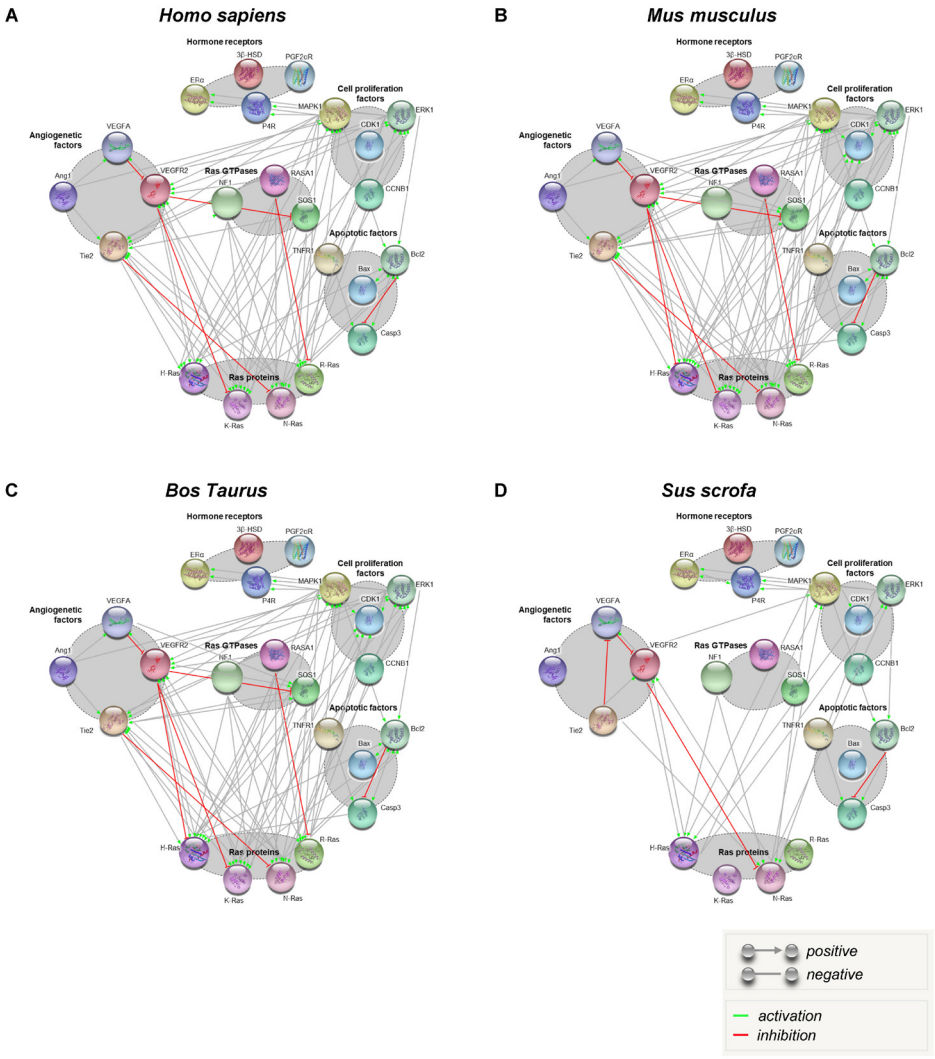


Fig. 4. Construction and analysis of the protein-protein interaction (PPI) network using the Search Tool for the Retrieval of Interacting Genes (STRING) database. Each edge color indicates a different method of PPI prediction. Network plot of top15 interaction protein in *Homo sapiens* (A), *Mus musculus* (B), *Bos Taurus* (C), and *Sus scrofa* (D). Proteins are represented as the respective national Center for Biotechnology Information (NCBI) gene names.

in *Homo sapiens* (Fig. 4A), *Mus musculus* (Fig. 4B), *Bos taurus* (Fig. 4C), and *Sus scrofa* (Fig. 4D) to compare conserved interaction patterns across major mammalian models. In the network, ERα was predicted to have a potential activating relationship with P4R (Fig. 4, green arrows), and ERα was also connected to the angiogenic module via VEGFA and its receptor VEGFR2. Additionally, the angiogenic receptors VEGFR2 and Tie2 were associated with Ras-related signaling through SOS1 (Fig. 4, green arrows), suggesting that these molecules may represent candidate links between angiogenic signaling and Ras-related pathways in porcine CL.

Moreover, the STRING molecular action map indicated that H-Ras and R-Ras were functionally connected to angiogenic receptors and SOS1, suggesting a potential network-level association between angiogenic signaling and Ras GTPase-related pathways (Fig. 4, green arrows). However, Ras GAP (NF1 and RASA1) were predicted to have inhibitory relationships with Ras signaling components (Fig. 4, red lines). Furthermore, Ras-related nodes were located at the interface between

https://doi.org/10.5187/jast.2600012

upstream hormone receptor/angiogenesis modules and downstream cell cycle (cell proliferation) factors (MAPK1, ERK1, CDK1, and CCNB1) via multiple interaction links (Fig. 4, gray lines). Contrastingly, apoptotic factors (TNFR1, Bax, Bcl2, and Casp3) were primarily connected within the apoptosis module and revealed relatively limited positive molecular interactions with hormone receptors, angiogenic factors, and Ras-related factors in the network (Fig. 4). Thus, although the overall architecture of these interaction modules is broadly conserved across four species, experimental evidence validating how these conserved connections operate in porcine CL is limited. Therefore, combining the species comparative network with stage-dependent expression profiles supports the requirement of porcine-specific studies to clarify the Ras-centered regulatory mechanisms coordinating angiogenesis, cell cycle transition, and luteal regression.

DISCUSSION

The CL is a transient endocrine tissue that undergoes rapid formation, functional maintenance, and regression during the estrous cycle, which requires the coordinated regulation of steroidogenesis, vascular remodeling, cell cycle transition, and apoptotic signaling [36,37]. Thus, we assessed stage-dependent variations in gross morphology and tissue weight, along with the expression profiles of steroid hormone receptor-related factors, angiogenesis- and cell cycle-related factors, apoptosis-related markers, and Ras-related components in the porcine CL, and further integrated these data using a STRING-based molecular action network.

Morphological features and tissue weight data indicated that the porcine CL reached its maximal growth during MP [38]. This observation was supported by 3β-HSD's expression pattern, which revealed the highest expression at the MP at the mRNA and protein levels [39]. This suggests that the MP corresponds to the period of improved steroidogenic capacity [40]. Additionally, *P4R* mRNA increased in the MP, whereas P4R protein increased in the EP. Although mRNA and protein levels do not always exhibit identical patterns, this discrepancy suggests that P4 signaling in porcine CL may be regulated at multiple levels, especially during early luteal development. Contrastingly, ERα did not exhibit considerable differences across estrous cycle at either the mRNA or protein level in the present dataset. This indicates that ERα expression itself may remain relatively stable during the estrous cycle. Notably, PGF2αR was the highest at the LP at the mRNA and protein levels, which is consistent with an elevated luteolytic responsiveness as the CL transitions toward regression [41]. Nevertheless, although the expression patterns of 3β-HSD and PGF2αR were consistent with the expected biological characteristics of MP and LP, respectively, 3β-HSD expression alone cannot be regarded as a direct measure of P4 production. Therefore, the interpretation of steroidogenic capacity based on 3β-HSD expression should be considered with caution. In future studies, particularly IHC-based analyses of Ras protein distribution in porcine CL tissues across the estrous cycle, P4 production in each sample will be quantified by ELISA to more accurately confirm the physiological status of the samples prior to further analysis.

Angiogenesis is necessary for CL formation and function, because the developing luteal tissue needs rapid vascularization and subsequent stabilization [17]. In the present study, the angiogenic factors exhibited marker- and level-dependent patterns. *VEGFA*, *VEGFR2*, and *Ang1* were analyzed at the mRNA level, whereas VEGFD and Ang4 was evaluated at the protein level, primarily due to practical considerations such as assay availability and antibody specificity. At the mRNA level, *VEGFA* and *VEGFR2* did not reveal considerable variations among the stages, whereas *Ang1* and *Tie2* were elevated in the MP. At the protein level, VEGFD was increased in the MP. Additionally, Ang4 and Tie2 protein did not reveal significant variations among the stages. Thus, luteal vascular

remodeling in pigs may be supported by distinct angiogenic mediators depending on the estrous cycle and molecular level. Additionally, the Ang-Tie axis and VEGF family members may contribute in a complementary but not identical way across development and regression.

With respect to cell cycle regulation, the mRNA expression of *ERK1*, *CDK1*, and *CCNB1* increased in the MP, whereas *MAPK1* mRNA did not significantly vary among the stages. However, at the protein level, ERK1/2 and p-ERK1/2 were not significantly different, whereas CCNB1 protein was increased in the EP. Although these patterns appear to be partially inconsistent at the molecular level, such variations can occur because complex regulatory steps, including translation efficiency, phosphorylation dynamics, and protein turnover, control cell cycle progression [42]. Therefore, the present findings indicate that the transcriptional activation of cell cycle regulators is prominent during MP, whereas protein level alterations may reflect earlier proliferative cues or differences in stability/processing during early luteal development.

Regarding apoptotic regulation, stage-dependent changes were noted that differed between transcripts and proteins. At the mRNA level, *TNFR1* increased in the LP, *Bax* and *Casp3* increased in the MP, and *Bcl2* increased in the EP. At the protein level, Casp3 was increased in the LP, whereas TNFR1, Bax, and Bcl2 did not reveal substantial differences during the estrous cycle. Thus, the transcriptional priming of apoptosis-related factors can be observed earlier; however, the execution marker (Casp3) becomes more evident at the protein level during LP, which is consistent with the structural regression occurring during luteolysis. Although not all apoptotic markers revealed substantial protein level alterations, the combined expression profiles support the concept that luteal regression involves a shift toward progressive signaling as the cell cycle progresses.

Ras-related signaling regulates cell proliferation, differentiation, and survival through pathways such as the MAPK/ERK pathway [43]. It reported that Ras and its GTPases genes dynamic are changed during estrous cycle in porcine cumulus cell [44], but estrous cycle regulation in porcine CL has not been clearly shown. Herein, Ras family members (H-, K-, N-, and R-Ras), Ras GEF (SOS1), and Ras GAP (NF1 and RASA1) revealed differential expression across the estrous cycle at the mRNA and protein levels. These data provide evidence that Ras-related components are dynamically regulated during the porcine estrous cycle and may be linked to luteal functional transition, especially during periods of rapid growth and functional maintenance. Although expression profiling alone does not confirm the direct activation states, these patterns support the requirement for further mechanistic validation of Ras-centered signaling in the luteal cells. Such mRNA-protein discordances observed across multiple targets in this study may be attributed to several study-specific factors, including post-transcriptional regulation, differences in protein turnover and stability between estrous phases, and tissue-level heterogeneity inherent to bulk CL samples composed of mixed luteal, vascular, and immune cell populations. In addition, sampling difference among individual CL and potential sensitivity limitation of estrous phase classification based on ovarian morphology may have contributed to the observed discrepancies. It should also be noted that the present study measured total receptor expression levels at the mRNA and protein level, which do not directly reflect receptor activation or transcriptional activity. Localization analyses such as immunohistochemistry (IHC) or immunofluorescence would be necessary to confirm cell-type-specific expression pattern and functional receptor engagement and are a priority for future studies.

Additionally, the STRING-based molecular action network provided an integrated framework for visualizing predicted functional associations among hormone receptor signaling, angiogenesis-related factors, cell-cycle modules, apoptosis-related nodes, and Ras-related factors. The same protein set was visualized in the same arrangement across *Homo sapiens*, *Mus musculus*, *Bos taurus*, and *Sus scrofa*. The network predicted potential associations among ERα-P4R, angiogenic receptors (VEGFR2

https://doi.org/10.5187/jast.2600012

and Tie2), the Ras activator SOS1, and Ras family proteins, whereas inhibitory relationships were predicted through NF1 and RASA1. Additionally, Ras-related nodes appeared to occupy intermediate network positions connecting the upstream hormone/angiogenesis modules with downstream cell cycle factors (ERK/MAPK-related nodes, CDK1, and CCNB1). Contrastingly, apoptosis-related factors showed revealed relatively limited positive molecular actions with the hormone receptor angiogenesis-Ras modules in the network. Thus, experimental validation in porcine luteal tissue is still limited, although the general architecture of these interactions is conserved across the four species. Additionally, porcine-specific studies are necessary to determine whether these Ras-centered regulatory mechanisms coordinate angiogenesis, cell cycle transition, and luteal regression in the CL.

Although the porcine CL used in this study were classified according to estrous phase, not all genes and proteins examined showed fully consistent phase-dependent patterns. This may partly reflect the biological heterogeneity of CL in polyovulatory pigs and the independent nature of samples collected from slaughtered animals. In future studies, including IHC-based analyses of Ras protein distribution in porcine CL tissues across the estrous cycle, P4 production in each sample will be measured by ELISA to more accurately confirm the physiological status of the samples before further analysis.

In summary, this study demonstrated that porcine luteal development and regression are accompanied by coordinated changes in morphology and tissue weight, stage-dependent expression patterns of steroid hormone receptors, and distinct profiles of angiogenesis, cell cycle, and apoptosis-related markers. Moreover, Ras family members change together with comparative network-based molecular actions. This suggests that Ras signaling may function as an integrative module that links endocrine and vascular cues to intracellular growth and survival pathways during the porcine estrous cycle. These results provide fundamental information for future studies aimed at validating Ras-related mechanisms in luteal cells and enhancing our understanding of luteal physiology in pigs.

CONCLUSIONS

This study showed clear phase-dependent alterations in the porcine CL during the estrous cycle, as evidenced by the morphology, tissue weight, and coordinated expression profiles of the key regulatory factors. CL demonstrated maximal growth at the MP, accompanied by increased *3β-HSD* expression, supporting improved steroidogenic capacity during functional maintenance. Contrastingly, PGF2αR expression was the highest at the LP, indicating elevated luteolytic responsiveness during regression. Overall, these results provide fundamental evidence that Ras-related signaling components are dynamically regulated in the porcine CL. Additionally, the findings support the requirement for porcine-specific mechanistic studies to clarify how endocrine and vascular cues coordinate luteal development and regression.

REFERENCES

1. Soede NM, Langendijk P, Kemp B. Reproductive cycles in pigs. Anim Reprod Sci. 2011;124:251-8. https://doi.org/10.1016/j.anireprosci.2011.02.025
2. Ziecik AJ, Przygrodzka E, Jalali BM, Kaczmarek MM. Regulation of the porcine corpus luteum during pregnancy. Reproduction. 2018;156:R57-67. https://doi.org/10.1530/REP-17-0662
3. Devoto L, Fuentes A, Kohen P, Céspedes P, Palomino A, Pommer R, et al. The human corpus luteum: life cycle and function in natural cycles. Fertil Steril. 2009;92:1067-79. https://doi.org/10.1016/j.fertnstert.2008.07.1745

4. Stocco C, Telleria C, Gibori G. The molecular control of corpus luteum formation, function, and regression. Endocr Rev. 2007;28:117-49. https://doi.org/10.1210/er.2006-0022
5. Selye H, Friedman SM. The action of various steroid hormones on the ovary. Endocrinology. 1940;27:857-66. https://doi.org/10.1210/endo-27-6-857
6. Hünigen H, Bisplinghoff P, Plendl J, Bahramsoltani M. Vascular dynamics in relation to immunolocalisation of VEGF-A, VEGFR-2 and Ang-2 in the bovine corpus luteum. Acta Histochem. 2008;110:462-72. https://doi.org/10.1016/j.acthis.2008.02.006
7. Brüssow KP, Schneider F, Nürnberg G. Alteration of gonadotrophin and steroid hormone release, and of ovarian function by a GnRH antagonist in gilts. Anim Reprod Sci. 2001;66:117-28. https://doi.org/10.1016/S0378-4320(01)00093-8
8. Christenson LK, Anderson LH, Ford SP, Farley DB. Luteal maintenance during early pregnancy in the pig: role for prostaglandin E2. Prostaglandins. 1994;47:61-75. https://doi.org/10.1016/0090-6980(94)90075-2
9. Jin X, Xiao LJ, Zhang XS, Liu YX. Apoptosis in ovary. Front Biosci. 2011;3:680-97. https://doi.org/10.2741/s180
10. Bertoli C, Skotheim JM, de Bruin RAM. Control of cell cycle transcription during G1 and S phases. Nat Rev Mol Cell Biol. 2013;14:518-28. https://doi.org/10.1038/nrm3629
11. Sun Y, Liu WZ, Liu T, Feng X, Yang N, Zhou HF. Signaling pathway of MAPK/ERK in cell proliferation, differentiation, migration, senescence and apoptosis. J Recept Signal Transduct Res. 2015;35:600-4. https://doi.org/10.3109/10799893.2015.1030412
12. Jochems R, Gaustad AH, Styrishave B, Zak LJ, Oskam IC, Grindflek E, et al. Follicular fluid steroid hormones and in vitro embryo development in Duroc and Landrace pigs. Theriogenology. 2022;190:15-21. https://doi.org/10.1016/j.theriogenology.2022.07.004
13. Billhaq DH, Lee S. The mechanisms of angiogenesis and apoptosis during the functional formation and regression of the corpus luteum in the ovarian reproductive endocrine system. Endocrines. 2025;6:53. https://doi.org/10.3390/endocrines6040053
14. Li D, Chen J, Guo J, Li L, Cai G, Chen S, et al. A phosphorylation of RIPK3 kinase initiates an intracellular apoptotic pathway that promotes prostaglandin2α-induced corpus luteum regression. eLife. 2021;10:e67409. https://doi.org/10.7554/eLife.67409
15. Lee SH, Lee S. Change of Ras and its guanosine triphosphatases (GTPases) during development and regression in bovine corpus luteum. Theriogenology. 2020;144:16-26. https://doi.org/10.1016/j.theriogenology.2019.12.014
16. Hennig A, Markwart R, Esparza-Franco MA, Ladds G, Rubio I. Ras activation revisited: role of GEF and GAP systems. Biol Chem. 2015;396:831-48. https://doi.org/10.1515/hsz-2014-0257
17. Plendl J. Angiogenesis and vascular regression in the ovary. Anat Histol Embryol. 2000;29:257-66. https://doi.org/10.1046/j.1439-0264.2000.00265.x
18. Min T, Lee SH, Lee S. Angiogenesis and apoptosis: data comparison of similar microenvironments in the corpus luteum and tumors. Animals. 2024;14:1118. https://doi.org/10.3390/ani14071118
19. Schwentner L, Wöckel A, Herr D, Wulff C. Is there a role of the local tissue RAS in the regulation of physiologic and pathophysiologic conditions in the reproductive tract? J Renin-Angiotensin-Aldosterone Syst. 2011;12:385-93. https://doi.org/10.1177/1470320311418140
20. Snoeren EMS. Female reproductive behavior. In: Coolen LM, Grattan DR, editors. Neuroendocrine regulation of behavior. Springer; 2019. p. 1-44.
21. Guthrie HD, Henricks DM, Handlin DL. Plasma estrogen, progesterone and luteinizing hormone prior to estrus and during early pregnancy in pigs. Endocrinology. 1972;91:675-9. https://doi.org/10.1210/endo-91-3-675

https://doi.org/10.5187/jast.2600012

22. Sykes M. Developing pig-to-human organ transplants. Science. 2022;378:135-6. https://doi.org/10.1126/science.abo7935
23. Mlyczyńska E, Kieżun M, Kurowska P, Dawid M, Pich K, Respekta N, et al. New aspects of corpus luteum regulation in physiological and pathological conditions: involvement of adipokines and neuropeptides. Cells. 2022;11:957. https://doi.org/10.3390/cells11060957
24. Längin M, Mayr T, Reichart B, Michel S, Buchholz S, Guethoff S, et al. Consistent success in life-supporting porcine cardiac xenotransplantation. Nature. 2018;564:430-3. https://doi.org/10.1038/s41586-018-0765-z
25. Woad KJ, Robinson RS. Luteal angiogenesis and its control. Theriogenology. 2016;86:221-8. https://doi.org/10.1016/j.theriogenology.2016.04.035
26. Przygrodzka E, Kaczmarek MM, Kaczynski P, Ziecik AJ. Steroid hormones, prostanoids, and angiogenic systems during rescue of the corpus luteum in pigs. Reproduction. 2016;151:135-47. https://doi.org/10.1530/REP-15-0332
27. Kurowska P, Mlyczyńska E, Dupont J, Rak A. Novel insights on the corpus luteum function: role of vaspin on porcine luteal cell angiogenesis, proliferation and apoptosis by activation of GRP78 receptor and MAP3/1 kinase pathways. Int J Mol Sci. 2020;21:6823. https://doi.org/10.3390/ijms21186823
28. Waterman RA. Lipid metabolism and in vitro production of progesterone and prostaglandin F during induced regression of porcine corpora lutea. Prostaglandins. 1980;20:73-85. https://doi.org/10.1016/0090-6980(80)90007-6
29. Seok E, Son M, Lee S, Cheong HT, Lee SH. The role of gonadotropins and growth factor in regulating Ras during maturation in cumulus–oocyte complexes of pigs. Animals. 2025;15:2100. https://doi.org/10.3390/ani15142100
30. Zhang Q, Wang Y, Bu Z, Zhang Y, Zhang Q, Li L, et al. Ras promotes germline stem cell division in Drosophila ovaries. Stem Cell Rep. 2024;19:1205-16. https://doi.org/10.1016/j.stemcr.2024.06.005
31. Therachiyil L, Anand A, Azmi A, Bhat A, Korashy HM, Uddin S. Role of RAS signaling in ovarian cancer. F1000Res. 2022;11:1253. https://doi.org/10.12688/f1000research.126337.1
32. Gao S, Wang J, Wei L, Luo C, Qian F, Bo L, et al. Trehalosemodulates OVRAS to improve oxidative stress and apoptosis in KGN cells and ovaries of PCOS mice. J Ovarian Res. 2024;17:11. https://doi.org/10.1186/s13048-023-01337-5
33. Sawada J, Urakami T, Li F, Urakami A, Zhu W, Fukuda M, et al. Small GTPase R-Ras regulates integrity and functionality of tumor blood vessels. Cancer Cell. 2012;22:235-49. https://doi.org/10.1016/j.ccr.2012.06.013
34. Livak KJ, Schmittgen TD. Analysis of relative gene expression data using real-time quantitative PCR and the 2−ΔΔCT method. Methods. 2001;25:402-8. https://doi.org/10.1006/meth.2001.1262
35. Snel B, Lehmann G, Bork P, Huynen MA. STRING: a web-server to retrieve and display the repeatedly occurring neighbourhood of a gene. Nucleic Acids Res. 2000;28:3442-4. https://doi.org/10.1093/nar/28.18.3442
36. Giacomini E, Pagliardini L, Minetto S, Pinna M, Kleeman F, Bonesi F, et al. The relationship between CYP19A1 gene expression in luteinized granulosa cells and follicular estradiol output in women with endometriosis. J Steroid Biochem Mol Biol. 2024;237:106439. https://doi.org/10.1016/j.jsbmb.2023.106439
37. Agca C, Ries JE, Kolath SJ, Kim JH, Forrester LJ, Antoniou E, et al. Luteinization of porcine preovulatory follicles leads to systematic changes in follicular gene expression. Reproduction. 2006;132:133-45. https://doi.org/10.1530/rep.1.01163

38. Mlyczyńska E, Zaobidna E, Rytelewska E, Dobrzyń K, Kieżun M, Kopij G, et al. Expression and regulation of visfatin/NAMPT in the porcine corpus luteum during the estrous cycle and early pregnancy. Anim Reprod Sci. 2023;250:107212. https://doi.org/10.1016/j.anireprosci.2023.107212
39. Chen G, Bourneuf E, Marklund S, Zamaratskaia G, Madej A, Lundstrom K. Gene expression of 3β-hydroxysteroid dehydrogenase and 17β-hydroxysteroid dehydrogenase in relation to androstenone, testosterone, and estrone sulphate in gonadally intact male and castrated pigs. J Anim Sci. 2007;85:2457-63. https://doi.org/10.2527/jas.2007-0087
40. Rasmussen MK, Ekstrand B, Zamaratskaia G. Regulation of 3β-hydroxysteroid dehydrogenase/Δ5-Δ4 isomerase: a review. Int J Mol Sci. 2013;14:17926-42. https://doi.org/10.3390/ijms140917926
41. Tanaka J, Acosta TJ, Berisha B, Tetsuka M, Matsui M, Kobayashi S, et al. Relative changes in mRNA expression of angiopoietins and receptors tie in bovine corpus luteum during estrous cycle and prostaglandin F2α-induced luteolysis: a possible mechanism for the initiation of luteal regression. J Reprod Dev. 2004;50:619-26. https://doi.org/10.1262/jrd.50.619
42. Glotzer M. The mechanism and control of cytokinesis. Curr Opin Cell Biol. 1997;9:815-23. https://doi.org/10.1016/S0955-0674(97)80082-8
43. Bradshaw T, Simmons C, Ott RK, Armstrong AR. Ras/MAPK signaling mediates adipose tissue control of ovarian germline survival and ovulation in Drosophila melanogaster. Dev Biol. 2024;510:17-28. https://doi.org/10.1016/j.ydbio.2024.02.009
44. Nam Y, Cheong HT, Lee SH. Changes of gonadotropin receptors and Ras subfamily genes during maturation in porcine cumulus cells. J Anim Reprod Biotechnol. 2025;40:50-7. https://doi.org/10.12750/JARB.40.1.50

https://doi.org/10.5187/jast.2600012